

---

This is an electronic reprint of the original article.  
This reprint may differ from the original in pagination and typographic detail.

Kujala, Pentti; Kõrgesaar, Mihkel; Kämäräinen, Jorma

## Evaluation of the limit ice thickness for the hull of various Finnish-Swedish ice class vessels navigating in the Russian Arctic

*Published in:*  
International Journal of Naval Architecture and Ocean Engineering

*DOI:*  
[10.1016/j.ijnaoe.2018.02.004](https://doi.org/10.1016/j.ijnaoe.2018.02.004)

Published: 01/05/2018

*Document Version*  
Publisher's PDF, also known as Version of record

*Published under the following license:*  
CC BY-NC-ND

*Please cite the original version:*  
Kujala, P., Kõrgesaar, M., & Kämäräinen, J. (2018). Evaluation of the limit ice thickness for the hull of various Finnish-Swedish ice class vessels navigating in the Russian Arctic. *International Journal of Naval Architecture and Ocean Engineering*, 10(3), 376-384. <https://doi.org/10.1016/j.ijnaoe.2018.02.004>

---

This material is protected by copyright and other intellectual property rights, and duplication or sale of all or part of any of the repository collections is not permitted, except that material may be duplicated by you for your research use or educational purposes in electronic or print form. You must obtain permission for any other use. Electronic or print copies may not be offered, whether for sale or otherwise to anyone who is not an authorised user.

Contents lists available at [ScienceDirect](#)

International Journal of Naval Architecture and Ocean Engineering

journal homepage: <http://www.journals.elsevier.com/international-journal-of-naval-architecture-and-ocean-engineering/>

## Evaluation of the limit ice thickness for the hull of various Finnish-Swedish ice class vessels navigating in the Russian Arctic

Pentti Kujala <sup>a, \*</sup>, Mihkel Kõrgesaar <sup>a</sup>, Jorma Kämäräinen <sup>b</sup>

<sup>a</sup> Aalto University, Department of Mechanical Engineering, PO Box 14300, FI-00076 Aalto, Finland

<sup>b</sup> Finnish Transport Safety Agency, Helsinki, Finland

### ARTICLE INFO

#### Article history:

Available online xxx

#### Keywords:

Loads

Serviceability

Limit ice thickness

Polar code

### ABSTRACT

Selection of suitable ice class for ships operation is an important but not simple task. The increased exploitation of the Polar waters, both seasonal periods and geographical areas, as well as the introduction of new international design standards such as Polar Code, reduces the relevancy of using existing experience as basis for the selection, and new methods and knowledge have to be developed. This paper will analyse what can be the limiting ice thickness for ships navigating in the Russian Arctic and designed according to the Finnish-Swedish ice class rules. The permanent deformations of ice-strengthened shell structures for various ice classes is determined using MT Uikku as the typical size of a vessel navigating in ice. The ice load in various conditions is determined using the ARCDEV data from the winter 1998 as the basic database. By comparing the measured load in various ice conditions with the serviceability limit state of the structures, the limiting ice thickness for various ice classes is determined. The database for maximum loads includes 3-weeks ice load measurements during April 1998 on the Kara Sea mainly by icebreaker assistance. Gumbel 1 distribution is fitted on the measured 20 min maximum values and the data is divided into various classes using ship speed, ice thickness and ice concentration as the main parameters. Results encouragingly show that present designs are safer than assumed in the Polar Code suggesting that assisted operation in Arctic conditions is feasible in rougher conditions than indicated in the Polar Code.

© 2018 Production and hosting by Elsevier B.V. on behalf of Society of Naval Architects of Korea. This is an open access article under the CC BY-NC-ND license (<http://creativecommons.org/licenses/by-nc-nd/4.0/>).

### 1. Introduction

IMO has adopted the International Code for Ships Operating in Polar Waters (Polar Code) and related amendments to make it mandatory under both the International Convention for the Safety of Life at Sea (SOLAS) and the International Convention for the Prevention of Pollution from Ships (MARPOL). One of the aspects of Polar Code addresses the operational limitations of ships of different categories (A, B and C) according to ice conditions. The approach for evaluating the ice conditions and setting limitations for ships assigned an ice class is called POLARIS – Polar Operational Limit Assessment Risk Indexing System, details of which are given in IMO amendment document (MSC 94, 2014). Therein the ice classes are associated with the limiting thickness by combining the experience from three existing approaches used in ice-covered

waters: the Canadian Arctic, Baltic (Finnish/Swedish), and Russian Northern Sea Route systems. The assessment given in MSC 94 (2014) categorizes ships designed according to Finnish Swedish Ice Class Rules (FSICR) for different operational conditions according to Table 1; assisted operation corresponds to scenario where icebreaker assistance is provided or the ice concentration is less than 100%.

Similarly, the objective of this work is to provide a limiting ice thickness for assisted operation, but through systematic evaluation of structural response to prescribed loads, which are later compared with actual measured loads. This will be achieved using numerical finite element simulations whereby permanent deformations of structures are determined along with the corresponding load level. Analysis are performed for three ice classes according to FSICR notation: IA Super, IA and IB. The permanent deformations comply with DNV serviceability limit state of  $s/12$  used by surveyors, Lepik et al. (2010). For the selected structure, long term measured data in different ice thicknesses is available meaning that we can associate the ice thickness with resulting

\* Corresponding author.

E-mail address: [pentti.kujala@aalto.fi](mailto:pentti.kujala@aalto.fi) (P. Kujala).

Peer review under responsibility of Society of Naval Architects of Korea.

<https://doi.org/10.1016/j.ijnaoe.2018.02.004>

2092-6782/© 2018 Production and hosting by Elsevier B.V. on behalf of Society of Naval Architects of Korea. This is an open access article under the CC BY-NC-ND license (<http://creativecommons.org/licenses/by-nc-nd/4.0/>).

**Table 1**  
Safe operation of ships in first-year winter ice regime for the Finnish-Swedish ice classes, MSC 94 (2014).

	Ice class	WMO description of the ice regime	Thickness of ice floes, At,
Assisted	IA Super	Medium first-year ice	$h_i$ , up to about 100 cm
	IA	Medium first-year ice	$h_i$ , up to about 80 cm
	IB	Thin first-year ice	$h_i$ , up to about 60 cm
	IC	Thin first-year ice	$h_i$ , up to about 40 cm

permanent deformation. The latter association lends itself to explicit definition of limiting ice thickness for safe operation.

**2. Case study**

As a case study, we selected M/T Uikku. Ship is classified according to DNV as class +1 A Tanker for Oil corresponding to FSICR as ice class IA Super. Ship was built 1976 in Werft Nobiskrug GmbH. Ship has a diesel electric propulsion system with four diesel generators. It is important to note that Uikku, in contrast to normal tanker, has a bow shape especially designed for operation in ice. The ship hull and propulsion system was instrumented on 1997 for the EU funded ARCDEV project and the instrumentation was extensive, detail description of the instrumentation can be found in Kotisalo and Kujala (1999) (see Fig. 1).

**2.1. Description of full scale measurements**

The ice load is measured on-board tanker M/T Uikku during one voyage to Ob-estuary in the Russian Arctic waters, from April to May in 1998. The voyage started from the port of Murmansk on 26th of April 1998, where the weather and ice conditions were harsh for the representative area. During the voyage M/T Uikku was

always either in convoy or lead by an icebreaker. The route of the convoy is presented in Fig. 2 (Kotisalo and Kujala, 1999). 20-minute maximum loads on-board M/T Uikku were measured in the bow, bow-shoulder and stern combined with visual observations. But since visual observations were not conveniently measured with the

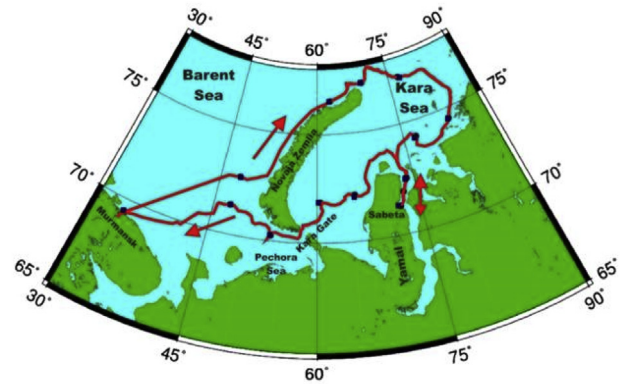


Fig. 2. Route of the convoy during ARCDEV voyage.

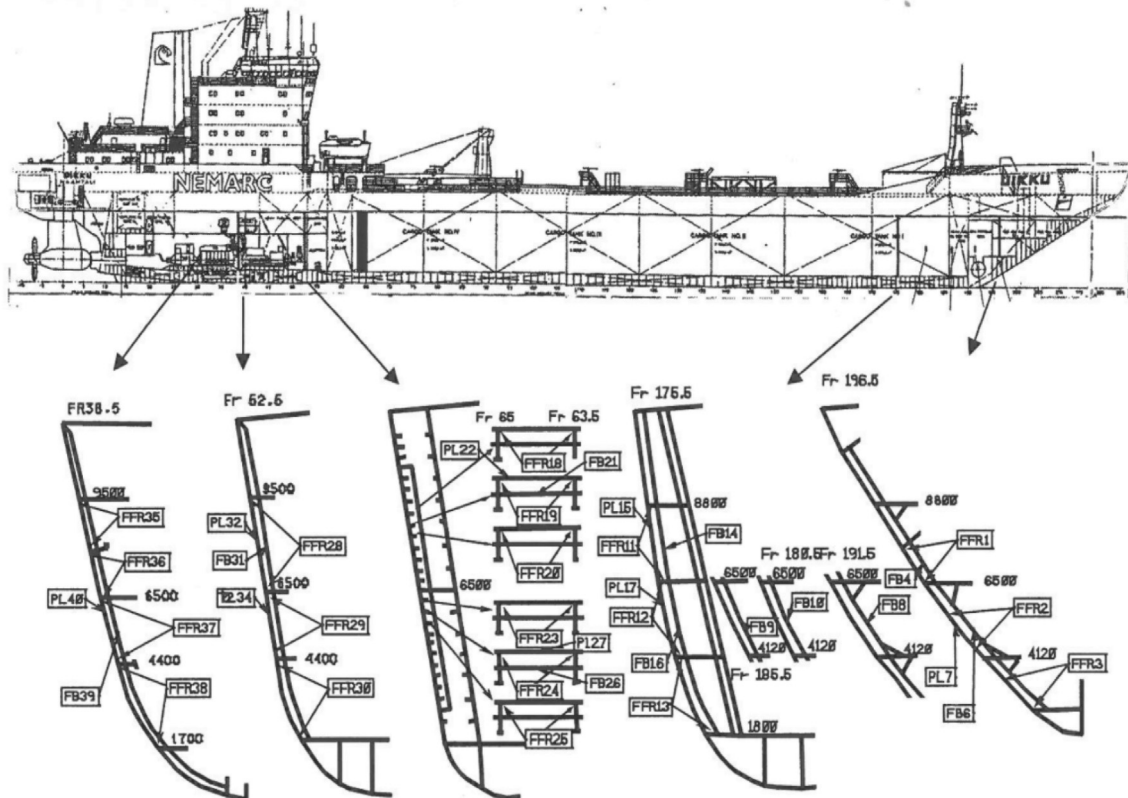


Fig. 1. Picture of Uikku showing the instrumented areas (Kotisalo and Kujala, 1999).

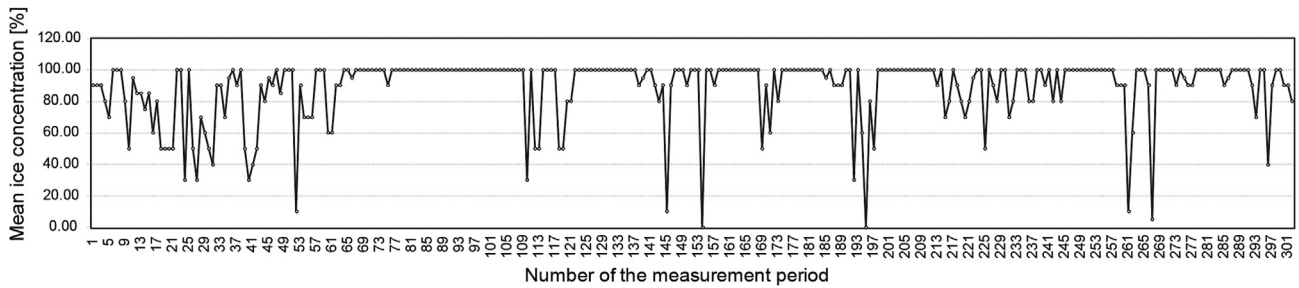


Fig. 3. Mean ice concentration in each observation period on-board MT Uikku.

same 20-min time interval as the loads, they were later synchronized. As the voyage was quite short only about 500 measured 20-min loads are available for the analysis. Based on the 500 measurements the time in those ice conditions per year was calculated to be about 7 days.

## 2.2. Observed ice conditions

Ice conditions were observed continuously by visual observations on the ship and reported in 20 min intervals. The ice concentration was observed in tenths during each observation period. The mean ice concentration during each observation period was calculated as a weighted average and the results are presented in Fig. 3.

Ice thickness was estimated by observing the thickness of the turning ice floes at the bow of the ship visually. Observations of ice thickness have been reported on five classes: below 10 cm, 10–30 cm, 30–70 cm, 70–120 cm and above 120 cm. Fig. 4 shows the observed mean ice thickness for each period. Fig. 5 shows the ship's speed during the voyage – due to the assisted operation the ship could keep a fairly high speed of 10–15 kn most of the time.

## 2.3. Return period of loads

The Gumbel I distribution is fitted to the ice load measurement data that is plotted in Fig. 6 as a function of return period. Gumbel I

distribution was used as it has proven to give a good fit to the data, see Kujala (1994), as well as because the initial distributions of the ice loads having an exponentially decaying tail (Gumbel, 1958). The cumulative distribution function of Gumbel I distribution is as follows, Ang and Tang (1984):

$$G(y_n) = \alpha_n e^{-e^{-\alpha_n(y_n - u_n)}} \quad (1)$$

where Gumbel parameter  $\alpha_n$  is the inverse measure of dispersion and  $u_n$  is the characteristic largest value. These are determined based on the mean  $\mu$  and standard deviation  $\sigma$  of the measured loads as follows:

$$\alpha_n = \frac{\pi}{\sigma\sqrt{6}} \quad (2)$$

$$u_n = \mu - \frac{\gamma}{\alpha_n} \quad (3)$$

Where  $\gamma = 0.577$  is the Euler constant. The measured 20-min maximum loads at the bow and stern are used in this analysis. The data is divided to three classes using ice thickness as the criteria: smaller than 0.7 m, between 0.7 and 1.2 m, and between 1.2 and 2.0 m. Fig. 6 summarise the measured load and fitted Gumbel I distribution on the data.

Fig. 6 shows that the load on the bow shoulder area is almost

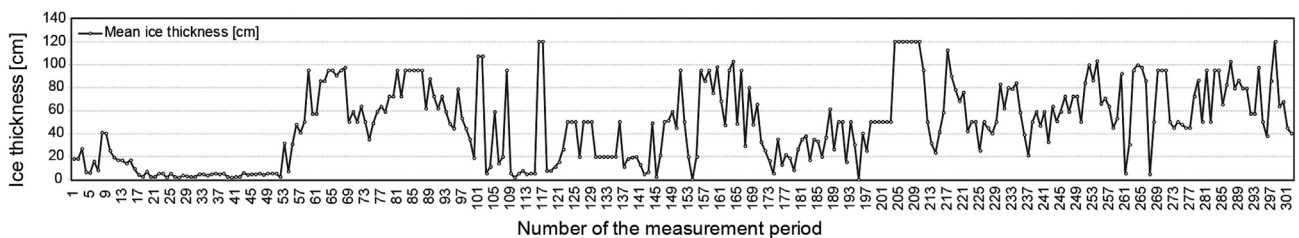


Fig. 4. Mean ice thickness in each observation period on-board MT Uikku.

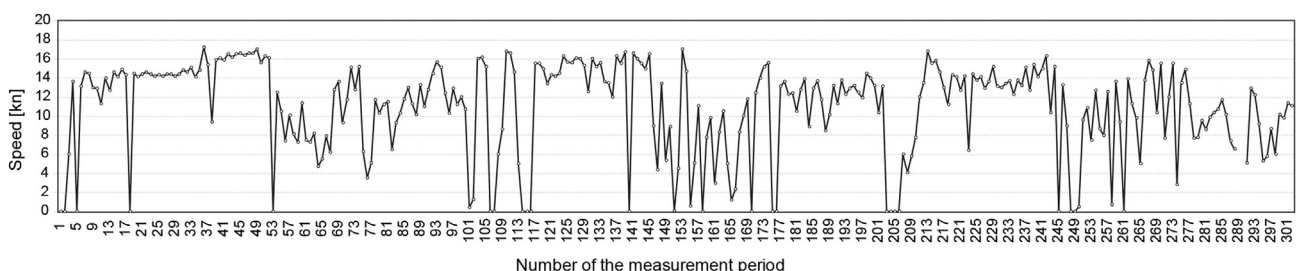


Fig. 5. The speed of MT Uikku during each 20-min period.

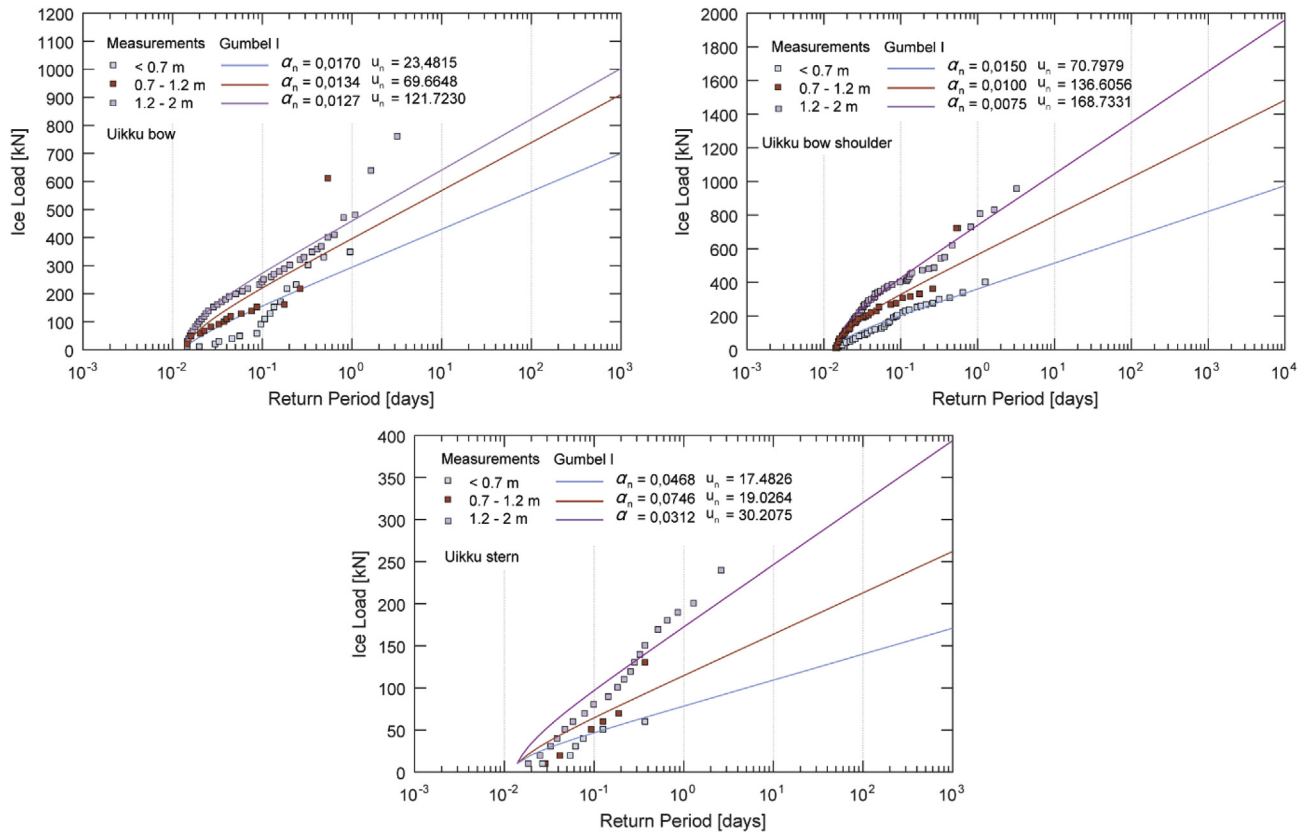


Fig. 6. Measure 20-min maxima with fitted Gumbel 1 distribution for MT Uikku from bow, bow shoulder and stern.

twice as high as on the bow area. The main reason for this is that the vertical frame angle is much smaller around the frame 176.5 (bow shoulder) than on the frame 196.5 (bow), which will result into higher ice induced loads to break the ice. In FSICR these areas are not separated, therefore in the following analysis, the load measured at the bow shoulder area will be used to evaluate the maximum ice thickness for various ice classes for the bow area. Another reason for the high load at the bow shoulder is that this area encountered more ice hits than the bow itself.

#### 2.4. Evaluation of design loads

The Gumbel fits provide the means to evaluate the extreme values with different probability levels. Therefore, using the Gumbel parameters  $\alpha_n$  and  $u_n$  the most probable extreme value with the probability of  $\alpha_s$  is given:

$$\widehat{y}_n = u - \alpha_n^{-1} \ln\left(-\ln\left(1 - \frac{\alpha_s}{n}\right)\right) \quad (4)$$

Using Eq. (4) and the data given in Fig. 6, the most probable design load values during one voyage, return period of one day, are given for two safety levels, namely  $\alpha_s = 0.1$  and  $\alpha_s = 1$ . Return period of one day was chosen as a compromise between data availability in lower ice thicknesses, about 3 days, and higher ice thickness, typically less than 1 day. The safety factor of  $\alpha_s = 1$  corresponds to one year extreme event which according to FSICR is yield. The factor  $\alpha_s = 0.1$  was chosen as it complies with the latest standard for design of Arctic offshore structures (ISO, 19906:2010), which defines the three exposure categories and related return period for the probability of occurrence of these:

1. Ultimate limit state (ULS) for all exposure levels (EL's) requires extreme 100-year ( $10^{-2}$ ) ice event with action factors dependent on the EL. ULS generally correspond to resistance to extreme applied actions.
2. Abnormal/accidental limit state (ALS) for with 1000-year ( $10^{-3}$ ) ice events allowing some structural damage, but robustness have to be achieved with no loss of life or harm to the environment.
3. Serviceability (SLS) ensuring functionality under any 10-year ( $10^{-1}$ ) ice event. Exceedance of SLS results in the loss of capability of a structure to perform adequately under normal use.

Ensuing probable design load values rising from the analysis of measured data must be associated with the structural response to provide the limiting ice thickness for safe operation. Therefore, structural response is determined in the following Section.

### 3. Analysis of structural response

#### 3.1. Scantlings

In order to assess the operational restrictions for different ice classes, Uikku's structural scantlings were re-calculated according to FSICR for three ice classes (IA Super, IA, and IB) and two hull regions, bow and stern, see Table 2. In calculations, the original built scantlings for the frame spacing, span and webframe spacing were used. In the bow, frame span is 2 m, 2.92 m in the bow-shoulder and 1.22 m in the stern; the frame spacing is 0.35 m for both regions. Webframe spacing was 2.8 m and 2.1 m, respectively, for bow and stern. In calculations, the minimum required engine power was calculated for IA and IB design according to FSICR requirements,

**Table 2**  
Uikku scantlings re-calculated for three ice classes, IA Super, IA and IB.

Bow	Plating	Frames [mm] (spacing = 0.35 m)				stringer [mm] (spacing = 2 m)				webframe [mm] (spacing = 2.8 m)				Power
	t [mm]	h web	t web	w flange	t flange	h web	t web	w flange	t flange	h web	t web	w flange	t flange	P [kW]
IAS	21.5	260	9.5	80	12.5	660	18	140	20	900	15	80	17	11400
IA	20	260	9	70	11.5	580	16	145	21	700	15	60	15	6614
IB	19	240	9	70	11.5	540	17	120	18	650	15	80	15	5300

Stem	Plating	Frames [mm] (spacing = 0.35 m)				stringer [mm] (spacing = 1.22 m)				webframe [mm] (spacing = 2.1 m)				Power
	t [mm]	h web	t web	w flange	t flange	h web	t web	w flange	t flange	h web	t web	w flange	t flange	P [kW]
IAS	14	120	9	40	11.5	450	8	60	14	500	10	80	16	11400
IA	11.5	100	9	50	10	340	8	80	14	380	10	80	16	6614
IB	10	80	9	40	10	290	10	40	10	290	10	40	10	5300

h\_web - web height [mm].

t\_web - web thickness [mm].

w\_flange - flange width [mm].

t\_flange - flange thickness [mm].

whereas for IA Super, the actual power of 11400 kW was used. All the stiffening members were assumed as T-shaped due to the modelling considerations explained below. The scantling calculations were automatized in the MATLAB routine.

### 3.2. Finite element modelling

All FE simulations were performed with FE software Abaqus/Standard 6.13–3. Modelled structures were discretized with reduced integration shell (S4R) elements with 5 integration points through thickness and stiffness based hourglass control. They possess six degrees of freedom on each node. Simulations were set-up using implicit analysis procedure (ABAQUS/Standard) using Static step, number of increments of 500 and minimum time increment of  $1e-12$ ; simulation time was 2 s. FE model generation based on input dimensions in Table 2 was automated with Abaqus python module.

Material true stress–strain relation is highly non-linear in the plastic region, but can be approximated as linear in the practical ranges of structural deformation of interest here as shown in Kõrgesaar et al. (2017). Therefore, a bi-linear elastic perfectly plastic

material was defined with the yield stress of 285 MPa.

Analyses are performed with a large 5-bay grillage structure shown in Fig. 7. To simplify the parametric modelling no brackets were modelled and structure was assumed perpendicular, i.e., without curvatures in the side shell. The reasoning behind the large model size was to reduce the effect of boundary conditions on the response. The edges of the model, including the cross-sections of the framing members as shown in Fig. 7, are restrained against translations. This is less conservative than fixing all degrees of freedom as stiffness is reduced. Moreover, the uncertainty related with boundary conditions is somewhat relieved by the large chosen model size.

### 3.3. Load definition

The definition of the ice load in combination with the corresponding strength criterion is the most important part of the hull rules. The load level and its distribution defines the structural response, which is basis for evaluation of the design point. The ice load in current rules is characterized with uniform pressure distributed over a patch with height depending on the ice class and length

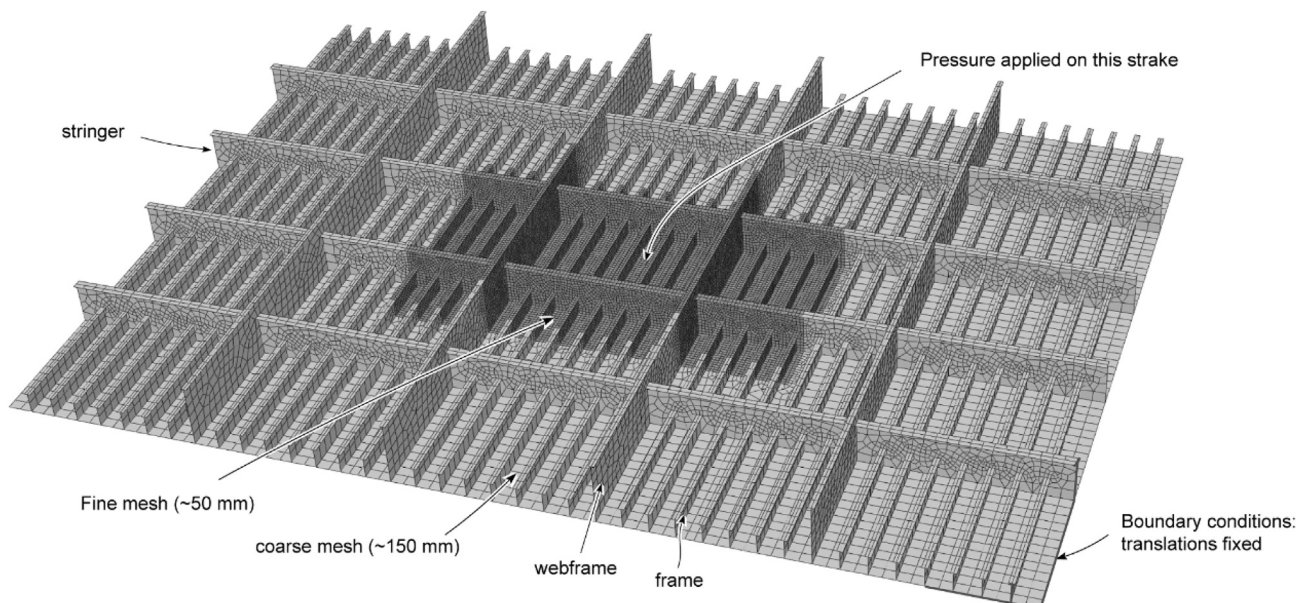


**Fig. 7.** 5-Bay grillage model used in the analysis. Scantlings correspond to IA Super bow region.

depending on the structural component to be dimensioned. In direct analysis using finite element method, the patch length is equal to the webframe spacing. However, a recent study by Körgesaar et al. (2017) showed that narrower patch as well as non-uniform distribution of pressure can inflict more damage to the structure. Important perspective considering that recent findings indicate that loads have to be narrow enough (1–4 frame spacings) in order for the maximum load on a frame to occur, Suominen et al. (2017).

Therefore, in this study following non-uniform pressure distribution is used for bow region:

$$p = \begin{cases} 4.35(7.175 - x)^{-0.733} & \text{if } x < 6.285 \\ 9.4 & \text{if } 6.825 \leq x \leq 7.175 \\ 4.35(x - 6.825)^{-0.733} & \text{if } x > 7.175 \end{cases} \quad (5)$$

where  $p$  is pressure in MPa and  $x$  is structural coordinate. Pressure on stern model is defined through similar equation:

$$p = \begin{cases} 2.9(5.775 - x)^{-0.733} & \text{if } x < 5.075 \\ 6.27 & \text{if } 5.075 \leq x \leq 5.425 \\ 2.9(x - 5.075)^{-0.733} & \text{if } x > 5.425 \end{cases} \quad (6)$$

This pressure profile is distributed over the area consistent with FSICR. The height of the patch is defined according to ice class: – IAS 0.35 m, IA 0.3 m, and IB 0.25 m. The length of the patch equals with webframe spacing that for bow region was 2.8 m and for stern region 2.1 m. The resulting pressure profiles are shown in Fig. 8 (a) and they are applied on a large grillage model between two middle webframes and stringers, i.e. on the centre strake as shown in Fig. 8 (c). The load is incrementally increased to the maximum value in the loading phase, and then gradually decreased in the unloading phase as shown in Fig. 8 (b). Similar procedure is advocated by the ABS (2014) guidance notes on ice class. Because of unloading, we could determine the permanent plastic deformation in the structure associated with serviceability limit state. Similar procedure is

advocated by the ABS (2014) guidance notes on ice class.

However, to reach the permanent displacement equal to  $s/12$ , the maximum pressure had to be chosen large enough so that sufficient permanent deformation would develop, although the load causing  $s/12$  deformation could not be defined a priori. Therefore, the unloading portion of the curve is shifted during the post-processing so that the permanent set would be equal to the reference permanent displacement as shown in Fig. 9. The underlying assumption is that slope of the unloading portion of the curve remains the same due to the permanent nature of plastic strains, whereas this assumption was validated with simulations with

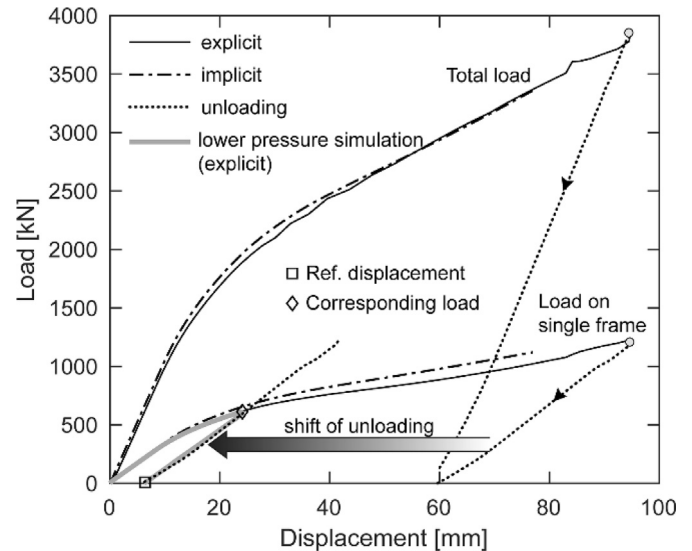


Fig. 9. Shifting of the unloading cycle to obtain permanent deformations. Total load corresponds to resultant force in the boundaries. Load on frame is obtained by integrating the pressure over the single frame spacing. Figure from Körgesaar et al. (2017).

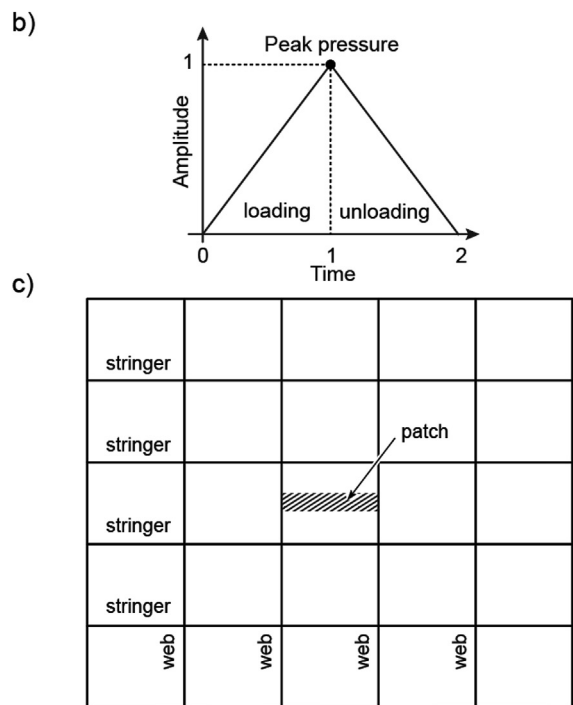
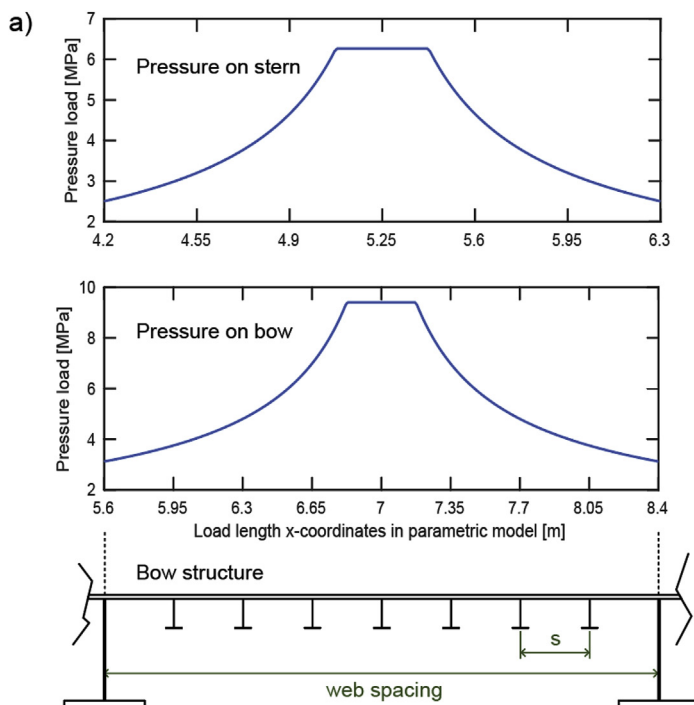


Fig. 8. a) Pressure distribution applied on structures showing the peak pressure value. B) The load amplitude with loading and unloading cycle. c) Pressure patch location on large grillage.

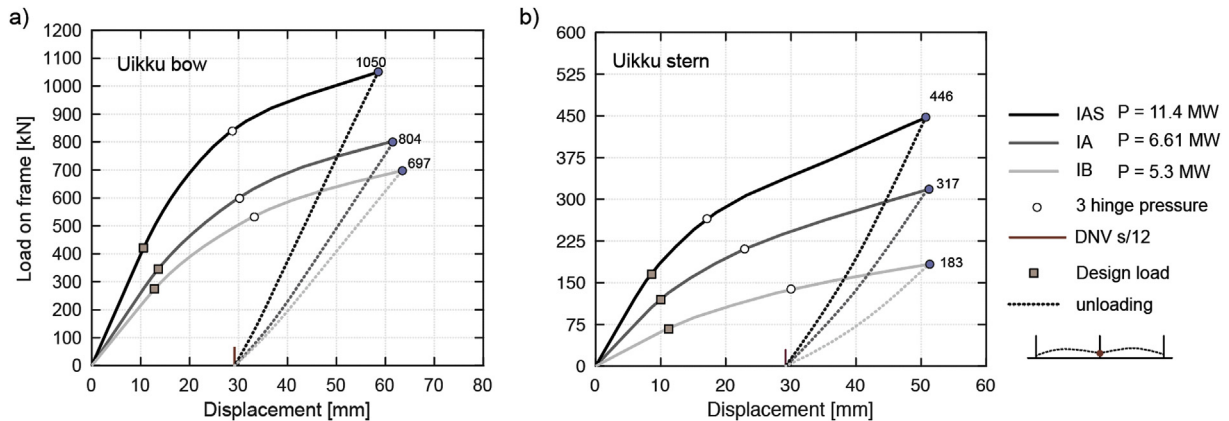


Fig. 10. Load-displacement relation for Uikku: a) bow region and b) stern region.

lower peak load in Kõrgesaar et al. (2017) and shown also in Fig. 9.

#### 4. Simulation results

The analysis results in Fig. 10 are presented in the form of load on single frame plotted as a function of displacement. The load on single frame was preferred over a total load as a comparative measure because measurement data also corresponds to single frames facilitating the comparison in the sequel. Load on single frame, that is for the one frame spacing, was found by integrating the applied pressure over the corresponding area. Displacements were measured in the plate field at the frame location.

Stiffness reduction of the frames in Fig. 10 correlates with the decrease in ice class as well as hull region – this is consistent with the current design approach. On the curves, three distinctive points are marked: load to permanent deformation  $s/12$ , design load according to FSICR and three hinge pressure load (Daley, 2002). The obtained results are gathered in Table 3.

The most captivating results in Table 3 are the safety factors against the yield load and permanent deformation load – for clarity, these are plotted on Fig. 11. The closer the safety factor is to one the more successfully the structure follows the design intention of FSICR that is reaching the state of yielding when subjected to design load. Both hull regions follow the design intention surprisingly well, while the stern region of IB class design might be slightly over-dimensioned with safety factor of 1.3 against yield. Similar consistency is observed in safety factors against permanent deformation with the value of  $\sim 2.5$  for all cases.

#### 5. Limiting ice thickness

Probable design load values complying with serviceability limit state ( $\alpha_s = 0.1$ ) are determined with Eq. (4) and compared with SLS

loads from structural analysis (Table 3) in Fig. 12. The measured data is plotted with markers at 0.7, 1.2, and 2 m, while dashed lines show the SLS load obtained with FE calculations.

Fig. 12 shows that bow shoulder loads are considerably higher than loads on bow. Since FSICR do not differentiate between bow regions, we use bow shoulder loads in comparison with loads obtained from FE analyses to be on the conservative side.

Therefore, IA Super design can operate in 2 m thick ice safely without sustaining damage equivalent to  $s/12$ , i.e.  $\sim 30$  mm, when icebreaker assistance is available. IA design can operate in 1.2 m and IB in 1 m thick ice.

In Fig. 13 the curves corresponding to  $\alpha_s = 1$  are plotted for reference to show the difference between 10 years and 1 year extreme event. Recall that FSICR design ships to yield once per winter, thus the Figure could be used as a gauge to estimate the compliance between design point and strength according to FSICR. The results are combined into Table 4 where the comparison is also presented with preliminary assessment made in POLARIS (MSC 94, 2014).

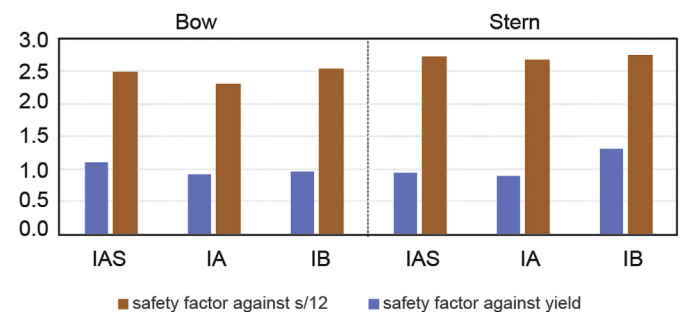


Fig. 11. Safety factors against yield and permanent deformation of  $s/12$ .

Table 3

Detailed analysis results for IA Super, IA and IB for two hull regions.

	BOW			STERN		
	IAS	IA	IB	IAS	IA	IB
Load for permanent deformation [kN]	1050	804	697	446	317	183
Yield limit [kN]	461	316	263	154	105	88
Patch area [m <sup>2</sup> ]	0.123	0.105	0.088	0.123	0.105	0.088
Design pressure [MPa]	3.44	3.31	3.13	1.34	1.13	0.76
Design load [kN]	421	348	274	164	119	67
p3h load [kN]	839	602	532	265	210	137
Safety factor against $s/12$	2.5	2.3	2.5	2.7	2.7	2.8
Safety factor against yield	1.1	0.9	1.0	0.9	0.9	1.3

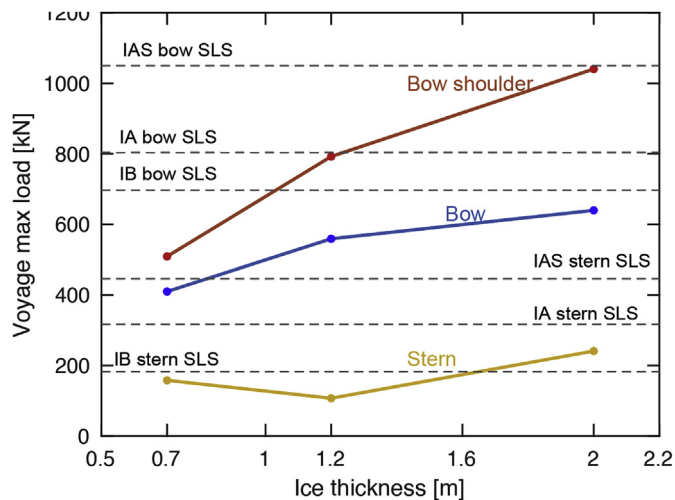


Fig. 12. Comparison of measured load with SLS load. Measured data corresponds to safety level of  $\alpha_s = 0.1$  (10 years extreme event).

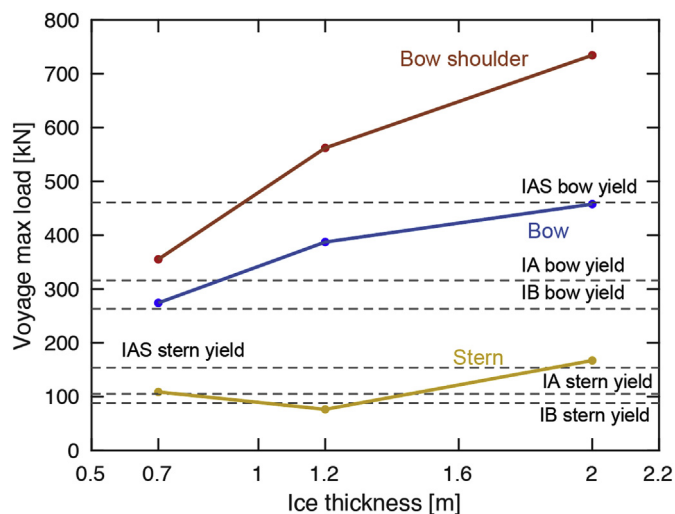


Fig. 13. Comparison of measured load with yield load. Measured data corresponds to safety level of 1 (1 years extreme event).

In POLARIS system, the operational restrictions are based on the definitions given in the Ice Nomenclature of WMO. Comparison reveals that preliminary assessment is more conservative, especially for the highest ice class. Systematic evaluation whereby measured data is compared with structural response analysis shows that IA Super can safely operate with icebreaker assistance or when ice concentration is less than 100% in 2 m ice without sustaining permanent damage of 30 mm – corresponding safe ice thickness according to POLARIS is half of that, 1 m. Preliminary assessment for IA and IB is less conservative with current analysis

yielding 50% and 67% higher safe ice thickness, respectively, for IA and IB class. Interestingly, the POLARIS assessment is much more consistent with the ice thicknesses corresponding to yield rather than the serviceability criteria.

6. Conclusions

Selection of suitable ice class for ships operation is an important, but not simple task. The increased exploitation of the Polar waters, both seasonal periods and geographical areas, as well as the introduction of new international design standards such as Polar Code, reduces the relevancy of using existing experience as basis for the selection, and new methods and knowledge must be developed.

This paper determined the limiting ice thickness for ships designed according to different ice classes of the Finnish-Swedish ice class navigating in the Russian Arctic. MT Uikku was used as the case study as the actual measurement data on-board ship was available. Thereby, the limiting ice thickness was determined by comparison of measured load in various ice conditions with the serviceability limit state of the structures established with FE simulations. Serviceability limit state corresponds to 10-year extreme event that was herein associated with a permanent deformation of  $s/12$ , i.e., 30 mm.

When serviceability is considered as a limiting condition for safe operation, results encouragingly show that present designs are safer than assumed in the Polar Code when operating under icebreaker assistance or when ice concentration is less than 100%. This extra safety depends on the ice class, with IA Super showing the largest safety margin. When conservatively associating yield with the safe operation, the limiting ice thicknesses provided by POLARIS correlates well with the present findings. Still, it is important to highlight the fact that Uikku has multifunctional icebreaking hull form which possibly decreases the measured loads. Nevertheless, results can be generalized to blunt hull forms as the largest measured loads are measured on the shoulder area, where the frame angle is not substantially different between multifunctional icebreaking hull and blunt hull. Another aspect that can affect the conclusions made in this study is the relevancy of used data. The data was gathered in 1998 and size of the MT Uikku is small compared with newly built shuttle tankers or LNG carriers operating in the same Russian Arctic. This uncertainty relates with balance between measured loads and increased structural scantlings.

Furthermore, there are two major, but opposing uncertainties in the results. First, pressure patch used in the analysis is a simplification and it excludes the development of line-like contact, which could have deteriorating effect on the capacity as shown in Ehlers et al. (2014), and Kujala and Kõrgesaar (2017). In other words, for the same nominal load, deformations would be higher, meaning that defined deformation limit would be reached earlier. Furthermore, the designed scantlings used in all ice classes were such that stable bending response was obtained during the loading, which implies large overload capacity. The overload capacity and

Table 4 Comparison between preliminary assessment from Polar Code and current results for safe operation of ships in first-year winter ice regime for the Finnish-Swedish ice classes, when icebreaker assistance is provided or the ice concentration is less than 100%.

POLARIS assessment (Polar Code)			Current assessment [cm]	
Ice class	WMO description of the ice regime	Thickness of ice floes, hi	SLS	Yield
IA Super	Medium first-year ice	hi up to about 100 cm	200 cm	100 cm
IA	Medium first-year ice	hi up to about 80 cm	120 cm	70 cm (some yielding)
IB	Thin first-year ice	hi up to about 60 cm	100 cm	50 cm (some yielding)
IC	Thin first-year ice	hi up to about 40 cm	–	–

permanent deformation limit could be reached earlier when more slender frames (but with the same section moduli) were adopted because of the consequent shift in deformation mode from bending the buckling (folding or tripping), Daley et al. (2017). Therefore, the effect of frame slenderness and how it affects permanent deformations should be further studied.

Second uncertainty is related to the definition of SLS criteria used in the analysis – permanent set of 30 mm. ISO standard for Arctic offshore structures (ISO, 19906:2010) relates exceedance of SLS with the loss of capability of a structure to perform adequately under normal use. Yet, observations of structural response at 30 mm indicate that there is additional reserve capacity before “adequate performance” is lost. Therefore,  $s/12$  of permanent set is believed to be conservative assumption for serviceability. In effect, we consider these two uncertainties to cancel each other rendering the results presented valid for the structures considered.

Conclusively, findings indicate that FSICR designs correlate well with the design point of yield, but large safety margin against permanent deformation limit indicates that further optimization of structures is possible.

### Acknowledgements

The financial support of the Lloyd's Register Foundation, United Kingdom, is acknowledged with gratitude. The Lloyd's Register Foundation helps to protect life and property by supporting engineering-related education, public engagement and the application of research. The support from Finnish Transport Safety

Agency (Trafi) is also acknowledged.

### References

- Ang, A.H.S., Tang, W.H., 1984. Probability Concepts in Engineering Planning and Design Volume II. John Wiley & Sons, New York.
- Daley, C.G., 2002. Derivation of plastic framing requirements for polar ships. *Mar. Struct.* 15, 543–559.
- Daley, C.G., Daley, K.H., Dolny, J., Quinton, B.W.T., 2017. Overload response of flatbar frames to ice loads. *Ships Offshore Struct.* 12, S68–S81.
- Ehlers, S., Erceg, B., Jordaan, I., Taylor, R., 2014. Structural analysis under ice loads for ships operating in arctic waters. In: Proceedings of the MARTECH2013.
- Gumbel, E., 1958. Statistics of Extremes. Columbia University Press, New York.
- ISO 19906, 2010. Petroleum and natural gas industries - arctic offshore structures. Section 7: Reliability and Limit State Design.
- Körgesaar, M., Kujala, P., Suominen, M., Dastydar, G.S., Kämäräinen, J., 2017. Effect of pressure distribution on the capacity of ship structure frames. In: Proceedings of the 6th International Conference on Marine Structures. MARSTRUCT 2017.
- Kotitalo, K., Kujala, P., 1999. Ice load measurements onboard MT Uikku during the ARCDEV voyage. In: Proceedings of the 15th International Conference on Port and Ocean Engineering under Arctic Conditions, pp. 974–987. August 23–27, Helsinki, Finland.
- Kujala, P., Körgesaar, M., 2017. Application of the Polar Code for the Finnish Swedish Ice Classes. Aalto University publication series SCIENCE + TECHNOLOGY; 02/2017, Aalto University, Finland (permanent web link will be provided with final submission).
- Kujala, P., 1994. On the Statistics of Ice Loads on Ship Hull in the Baltic. Doctoral Thesis. Helsinki University of Technology, Espoo.
- Lepik, K., Peetsalu, J., Viljakainen, S., Voog, V., 2010. Allowable Plate Deflections According to DNV. Internal instructions for surveyors.
- MSC 94, 2014. IMO Maritime Safety Committee/INF.13, Technical Background to POLARIS.
- Suominen, M., Kujala, P., Romanoff, J., Remes, H., 2017. Influence of load length on short-term ice load statistics in full-scale. *Mar. Struct.* 52, 153–172. <https://doi.org/10.1016/j.marstruc.2016.12.006>.